

Nigerian Journal of Engineering Science Research (NIJESR). Copyright@ Department of Mechanical Engineering, Gen. Abdusalami Abubakar College of Engineering, Igbinedion University, Okada, Edo State, Nigeria.

ISSN: 2636-7114





Advanced Computational Methods for predicting Evaporation Rate of Fe Alloys during Weld Pool Formation

^{1a}Nicholas Chika Ogu, ^{1b}Joseph Ifeanyi Achebo, ^{2c}Kessington Osahenrumwen Obahiagbon, ^{1d}Frank Omos Uwoghiren, ^{1e}Andrew Ozigagun

¹Department of Production Engineering, Faculty of Engineering, University of Benin, Benin City, Nigeria ²Department of Chemical Engineering, Faculty of Engineering, University of Benin, Benin City, Nigeria

Corresponding Author's: Nicholas Chika Ogu; chikaeze1000@yahoo.com

Manuscript History Received: 18/12/2024 Revised: 24/02/2025 Accepted: 12/04/2025 Published: 20 /04/2025 https://doi.org/10.5281/ zenodo.17410310

Abstract: The present study addresses the challenge of optimizing welded parameters to achieve optimal Fe content by employing expert models in developing an optimal combination of input parameters for high-quality Fe welds using ungsten inert gas (TIG) welding. An optimal randomized matrix is developed using the central composite design, setting-up the input factors such as the weld current, voltage, and gas flow rate for each experimental run. Response Surface Methodology (RSM) and Artificial Neural Network (ANN) were utilized for experimental analysis. The RSM approach yielded a mathematical model for optimizing process parameters, following satisfactory diagnostic tests such is lack of fit test, sequential sum of squares, goodness of fit, analysis of variance, and surface plots. The optimal solution resulted in a current of 185 A, voltage of 20 V, and gas flow rate of 16 L/min, producing a weldment with a Fe content of 96.484. ANN evaluation metrics results of R² values, 0.9498 were compared with RSM-prediction results, R² values of 0.9699. The result showed the RSM outperformed the ANN in effectively modelling and predicting the Fe content.

Keywords: Welding, Iron (Fe), Central composite design, Weld Quality, Alloys

INTRODUCTION

Welding is a vital process in manufacturing and construction, and it relies heavily on the behavior of metals during the welding process (Zhang et al., 2020). The evaporation of iron (Fe) alloys is a critical aspect of welding that affects the quality of the weld joint [2]. The temperature of the droplets formed during the welding process plays a crucial role in influencing the evaporation rates of Fe alloys as they interact with the molten weld pool (Zhu et al., 2018). Understanding and controlling this process is essential for optimizing welding parameters and achieving high-quality welds. The evaporation of Fe alloys during welding is influenced by various factors, including temperature, alloy composition, and welding parameters (Ghaini et al., 2020). The temperature of the droplets that form during welding is particularly important (Mamat et al., 2018; Cho et al., 2021). Researchers have conducted numerous experimental studies to measure and analyze the evaporation rates of Fe alloys under various welding conditions (Chen et al., 2018), as analytical decision-support frameworks, coupled with advanced computational methods, enable data-driven insights that improve operational efficiency and facilitate informed optimization strategies (Ovejide et al., 2018). The studies use specialized equipment and techniques to monitor alloy evaporation in real-time (Baehr et al., 2018), in which data collected provides valuable insights into the evaporation process and its impact on weld quality (Martin et al., 2019). Predicting and optimizing evaporation rates during welding is crucial for achieving consistent and high-quality welds (Fotovvati et al., 2018) as integrated modelling strategies have proven to have enhanced reliability and practical relevance (Oyejide et al., 2025). Mathematical models and simulations have been developed to account for variables such as droplet temperature, alloy composition, and heat input.

The evaporation rates of Fe alloys have a significant impact on the quality and integrity of welds (Cadiou et al., 2020; Chen et al., 2020). Excessive evaporation can lead to defects such as porosity and inclusions, which compromise weld quality (Bunazivm et al., 2021). By optimizing evaporation rates, it is possible to produce welds with improved mechanical properties and enhanced performance (Indhu et al., 2018; Bunazivm et al., 2021; Zhang et al., 2022). Paul and Dhar (2024) developed a comprehensive machine learning framework to predict sessile droplet evaporation kinetics including the evaporation rate, temperature drop and velocity scale, given some set of conditions. They employed deep artificial neural network (ANN), random forests (RF), and extreme gradient boosting (XGB) models. Their approach involved cascading output features based on underlying physics, which improved prediction accuracy. ANN was superior to others, with a lesser mean absolute error for the majority of the target variables. The study showed that ML models, in particular ANNs, can predict the droplet evaporation parameters in a physically-consistent manner and can be considered a computationally cheaper alternative to full numeric simulations. Rawa et al. (2023) introduced a hybrid method that merges numerical simulations with particle-swarm-optimized artificial neural networks to analyse the thermal behaviour and melting ratio in pulsed laser welding of stainless-steel alloys. The numerical simulations elucidated how variations in pulse duration and frequency modulate the temperature and velocity fields, with Marangoni and buoyancy forces emerging as critical contributors. Using an ANN whose topology and learning parameters were refined by Particle Swarm Optimization (PSO), it achieved low-error, for the maximum temperature and melting ratio across training, validation, and test datasets. This hybrid approach enabled accurate, and faster prediction of key thermal parameters in welding processes. Zhang et al. (1993) developed a three-dimensional finite volume model designed to replicate fluid flow, droplet transfer, and keyhole dynamics during laser-MIG hybrid welding of the Fe36Ni Invar alloy. The approach employed double-ellipsoidal heat distributions for the arc and an adaptive Gauss rotary source for the laser, while also incorporating recoil pressure, electromagnetic and Marangoni effects, and buoyancy forces. Comparisons with experimental data showed that the model reliably reproduced temperature distributions and final weld profiles, yielding valuable information for refining welding parameters of Fe alloys. Despite advancements in understanding alloy evaporation, challenges remain. The behavior of Fe alloys at high temperatures is complex, and further research is needed to fully understand and control the process (Wang et al., 2023). Accurate data and advanced modeling techniques are required to improve predictive capabilities (Kaiser et al., 2018). Future research may focus on developing new welding methods and technologies that offer greater control over alloy evaporation. Optimizing and predicting evaporation rates of Fe alloys influenced by droplet temperature during weld pool formation is essential for advancing welding technology and improving weld quality. The complex relationship between droplet temperature and alloy evaporation underscores the importance of this area of study. Ongoing research continues to refine welding processes and enhance the quality of welds, contributing to the development of more reliable and efficient manufacturing and construction methods.

The key contributions of the present study are as follows:

- i. This research introduces a robust computational framework for optimising and predicting the evaporation rates of Fe alloys during welding, as a function of the droplet temperature. The model is developed based on RSM and ANN, which provides the ability to capture non-linear relationship in weld pool dynamics and enhances the accuracy of prediction as well as understanding the process.
- ii. The findings indicated that the model developed using RSM provided an accurate fit to experimental data, as indicated by high R² values, and favourable goodness of fit diagnostics, including predicted and adjusted R² in close agreement and an adequate signal-to-noise ratio. Simultaneously the implementation of ANN demonstrated the capability of machine learning to capture complex patterns in the dataset, offering a computationally efficient alternative to traditional physical simulations for forecasting key welding response variables.
- iii. The reliability and robustness of the established models were verified by model diagnostics such as lack of fit tests, residual analysis, and Cook's distance analysis. This systematic approach establishes a dependable predictive tool for weld quality optimization, directly supporting enhanced operational control and defect minimization in Fe alloy welding applications.

The remaining sections of this paper is organised as follows. Section 2 describes the experimental design, which includes the selection of input parameters, experimental setup, and the development of both RSM and ANN models. Section 3 presents the results and discussion, featuring an in-depth assessment of model performance, diagnostic plots, and comparison of predictive accuracy between the proposed computational methods. Section 4 concludes the study by outlining the implications of the findings, potential applications for quality assurance in welding processes, and recommendations for future research to further refine computational modelling of alloy evaporation dynamics.

MATERIALS AND METHODS

2.1 Design of Experiment

Design of Experiments (DOE) is a powerful analysis tool for modelling and analyzing the influence of multiple control factors on the performance output. DOE refers to planning, designing and analyzing an experiment so that valid and objective conclusions can be drawn effectively and efficiently. If a certain quality feature of a product, the response, is being affected by many variables, the best strategy is then to design an experiment in order to achieve valid, reliable and sound conclusions in an effective, efficient and economical manner. It is important to know that some factors may have strong effects on the response, others may have moderate effects and some have no effects at all. In manufacturing, experiments are conducted to improve the understanding and knowledge of different engineering processes with the aim of producing high quality products.

2.2 Materials Selection and Welding Equipment

The material selected for this experiment is a mild steel plate. Mild steel is widely applied in the manufacture of different engineering structures. It is very much available and affordable. The physical properties and base metal chemistry of mild steel is suitable for most engineering needs. The tungsten inert gas welding process is chosen because it produces a homogenous weld joint. TIG welds are strong and possess relatively high corrosion resistance compared to other metals. Mild steel plate of thickness 10 mm was selected as material used for the experiment. The mild steel plate was cut with dimension of 60 mm x 40 mm with the help of power hacksaw and grinded at the edge to smoothen the surfaces to be joined. The surfaces of the coupon were polished with emery paper, thereafter the mild steel plates were fixed on the work table with flexible clamp to weld the joints of the specimen. A TIG welding process was used with Alternate Current (AC) to perform the experiments as it concentrates the heat in the welding area, using 100% argon gas as the shielding gas. For each experimental runs 5 specimen was used, and the average of the 5 experimental readings were recorded for the 20 runs.

2.3 Response Surface Methodology

RSM Engineers often search for the conditions that would optimize the process of interest. In other words, they want to determine the values of the process input parameters at which the responses reach their optimum. The optimum could be either a minimum or a maximum of a particular function in terms of the process input parameters. RSM is one of the optimization techniques currently in widespread usage to describe the performance of the welding process and find the optimum of the responses of interest. RSM is a set of mathematical and statistical techniques that are useful for modelling and predicting the response of interest affected by several input variables with the aim of optimizing this response (Kim *et al.*, 2025). RSM also specifies the relationships among one or more measured responses and the essential controllable input factors. RSM is used to develop empirical model, commonly called response surface, for the response of a process in terms of the relevant controllable factors (Veza *et al.*, 2023). RSM determines the operating conditions that produce the optimum response. Response Surface Methodology allows you to specify and fit a model up to the second order, RSM fits a model and provides the ANOVA and the 'Lack of Fit' test separately when there is more than one response. Contour and Surface plots of each response for pairs of factors are also produced. The aim of the response surface are to help understand the topography of the surface plot using simple maximum or minimum, saddles and ridges 3D diagrams and to find the region with the optimum response using contour plots.

2.4 Artificial Neural Networks

Neural network are data mining tool for finding unknown patterns in databases, a neural network is a massively parallel distributed processor that has a natural propensity for storing experimental knowledge and making it available for use (Lian and Chen, 2024). It resembles the brain in two respects. Knowledge is acquired by the network through a learning process, Interneuron connection strengths known as synaptic weights are used to store the knowledge. An elementary neuron with R input is weighted with an appropriate w. The sum of the weighted inputs and the bias forms the input to the transfer function f (Abiodun *et al.*, 2019). Neurons can use any differentiable transfer function f to generate their output. Multilayer networks often use the log-sigmoid transfer function logsig.

RESULTS AND DISCUSSION

3.1 Modelling and Prediction using Response Surface Methodology (RSM)

In this study, twenty experimental runs were carried out, each experimental run comprising the current, voltage and gas flow rate, used to join two pieces of mild steel plates measuring 60 x 40 x 10mm. The Fe was measured respectively. In validation of the suitability of the quadratic model in analyzing the experimental data, the sequential model sum of squares was calculated for Fe content responses as presented in Table-1.

Table-1 Sequential model sum of square for Fe

Source	Sum of Squares	df	Mean Square	F-value	p-value	
Mean vs Total	1.678 x 10 ⁵	1	1.678 x 10 ⁵			
Linear vs Mean	154.36	3	51.45	1.67	0.2130	
2FI vs Linear	100.00	3	33.33	1.10	0.3827	
Quadratic vs 2FI	372.98	3	124.33	63.90	< 0.0001	Suggested
Cubic vs Quadratic	2.64	4	0.66	0.24	0.9086	Aliased
Residual	16.82	6	2.80			
Total	1.685×10^5	20	8422.90			

The sequential model sum of squares table shows the accumulating improvement in the model fit as terms are added. Based on the calculated sequential model sum of square, the highest order polynomial where the additional terms are significant and the model is not aliased was selected as the best fit. From the results of Table 1, it was observed that the cubic polynomial was aliased hence cannot be employed to fit the final model. In addition, the quadratic and 2FI model were suggested as the best fit thus justifying the use of quadratic polynomial in this analysis. In testing how well the quadratic model can explain the underlying variation associated with the experimental data, the lack of fit test was estimated for each of the responses. Model with significant lack of fit cannot be employed for prediction. Results of the computed lack of fit for the Fe is presented in Table-2.

Table-2 Lack of fit test for Fe

Source	Sum of Squares	df	Mean Square	F-value	p-value	
Linear	477.11	11	43.37	14.14	0.0045	
2FI	377.11	8	47.14	15.37	0.0040	
Quadratic	4.12	5	0.8244	0.2688	0.9122	Suggested
Cubic	1.48	1	1.48	0.4835	0.5178	Aliased
Pure Error	15.33	5	3.07			

The results of Table 2 shows that the quadratic polynomial had a non-significant lack of fit and was suggest for model analysis while the cubic polynomial had a significand lack of fit hence aliased to model analysis. The model statistics computed for Fe response based on the model sources is presented in Table 3.

Table-3 Model summary statistics for Fe

Source	Std. Dev.	R ²	Adjusted R ²	Predicted R ²	PRESS	
Linear	5.55	0.2387	0.0959	-0.1398	737.23	
2FI	5.49	0.3933	0.1132	-0.5787	1021.12	
Quadratic	1.39	0.9699	0.9428	0.9176	53.30	Suggested
Cubic	1.67	0.9740	0.9177	0.4605	348.92	Aliased

The summary statistics of model fit shows the standard deviation, the r-squared, adjusted r-squared, predicted r-squared and predicted error sum of square (PRESS) statistic for each complete model. Low standard deviation, R-Squared near one and relatively low PRESS is the optimum criteria for defining the best model source. Based on the results of Table-3, the quadratic polynomial model was suggested while the cubic polynomial model was aliased hence, the quadratic polynomial model was selected for this analysis. In validating the adequacy of the quadratic model based on its ability to minimize the Fe content, the goodness of fit statistics is presented in Table-4.

Table-4 Goodness of Fit Statistics for Fe

Std. Dev.	1.39	\mathbb{R}^2	0.9699
Mean	91.60	Adjusted R ²	0.9428
C.V. %	1.52	Predicted R ²	0.9176
		Adeq Precision	19.2951

The Predicted R² of 0.9176 is in reasonable agreement with the Adjusted R² of 0.9428; i.e. the difference is less than 0.2. Adeq Precision measures the signal to noise ratio. A ratio greater than 4 is desirable. The ratio of 19.295 indicates an adequate signal. This model can be used to navigate the design space. In accepting any model, its satisfactoriness must first be checked by an appropriate statistical analysis output. To diagnose the statistical properties of the response surface model, the normal probability plot of residual presented in Fig. 1.

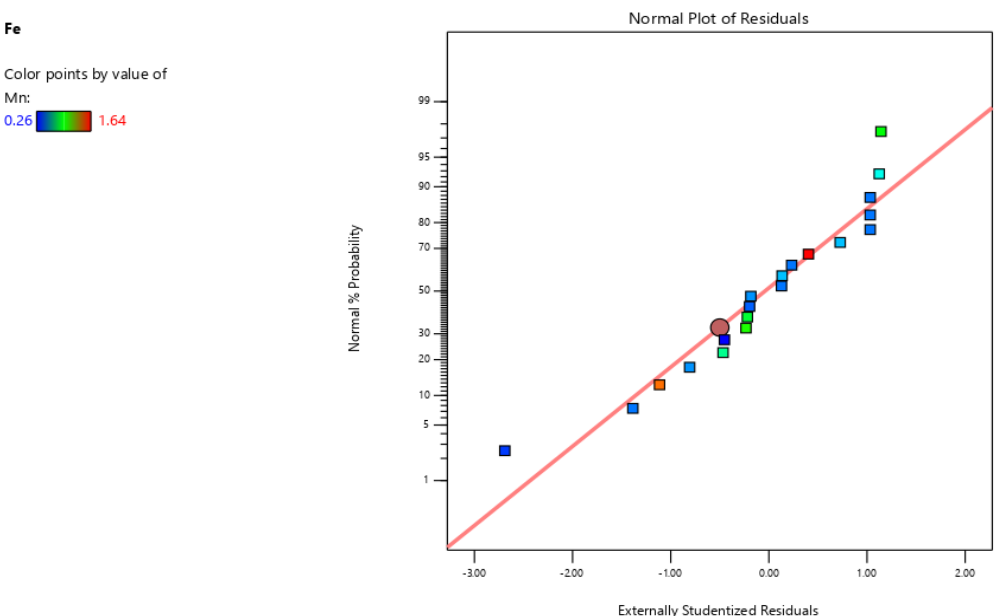


Fig.1 Normal probability plot of studentized residuals for Fe

It can be observed that the points follow a straight line despite the slight scatter. There is no defined pattern like an 's-shaped' curve aside from the linear trend. This indicates that the residuals are normally distributed and no transformation of the response data is required for better analysis. The normal probability plot of studentized residuals was employed to assess the normality of the calculated residuals. The normal probability plot of residuals, which is the number of standard deviations of actual values based on the predicted values was employed to ascertain if the residuals (observed - predicted) follows a normal distribution. It is the most significant assumption for checking the sufficiency of a statistical model. Result of Fig. 1 revealed that the computed residuals are approximately normally distributed an indication that the model developed is satisfactory. A plot of residuals and the predicted to detect the presence of mega patterns or expanding variance was produced for Fe which is shown in Fig. 2.

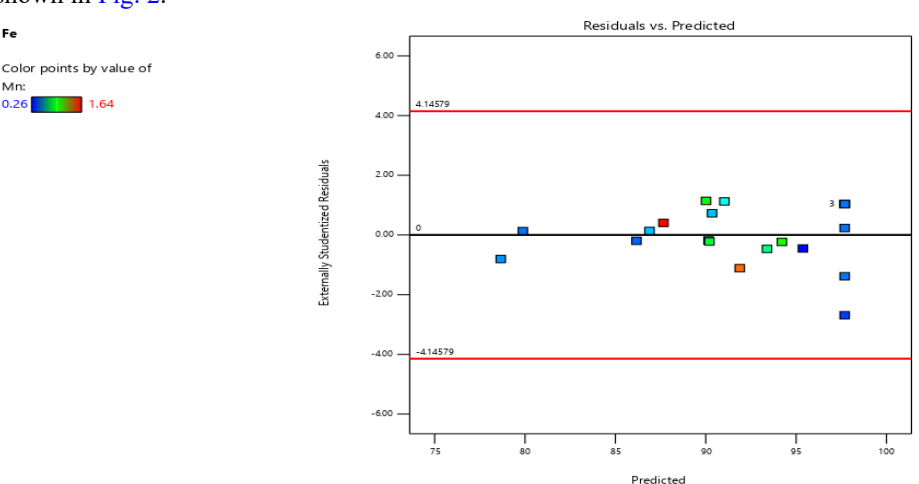


Fig. 2 Plot of Residual vs Predicted for Fe

As can be observed, the graph is a random scatter indicating a range of constant residuals across the graph. In order to detect a value or group of values that are not easily detected by the model, the predicted values are plotted against the actual values, for Fe content which is shown in Fig. 3.

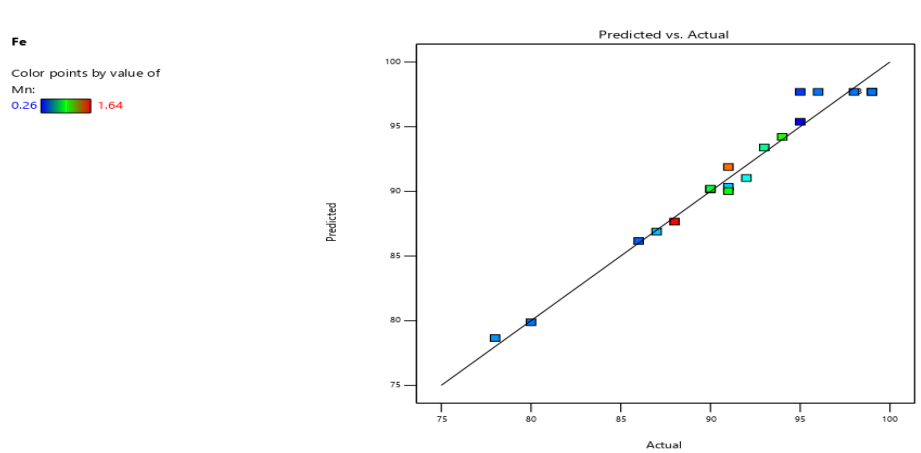


Fig. 3 Plot of Predicted Vs Actual for Fe

As can be seen from the graph, the points are close to the line of fit. The model essentially is able to predict most of the data points. In determining the presence of a possible outlier in the experimental data, the cook's distance plot was generated for the different responses. The cook's distance is a measure of how much the regression would change if the outlier is omitted from the analysis. A point that has a very high distance value relative to the other points may be an outlier and should be investigated. The generated cook's distance for Fe is presented in Fig. 4.

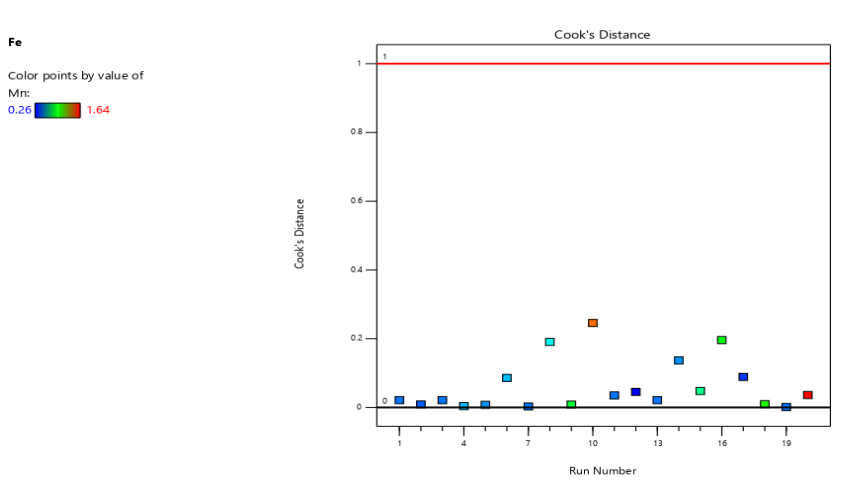


Fig. 4 Generated cook's distance for Fe

The cook's distance plot has an upper bound of 1.00 and a lower bound of 0.00. Experimental values smaller than the lower bound or greater than the upper bounds are considered as outliers and must be properly investigated. Results of Figure 4 indicate that the data used for this analysis are devoid of possible outliers thus revealing the adequacy of the experimental data. In studying the effects of combined current and voltage on the Fe content, 3D surfaces plots presented in Fig. 5 was generated as follows.

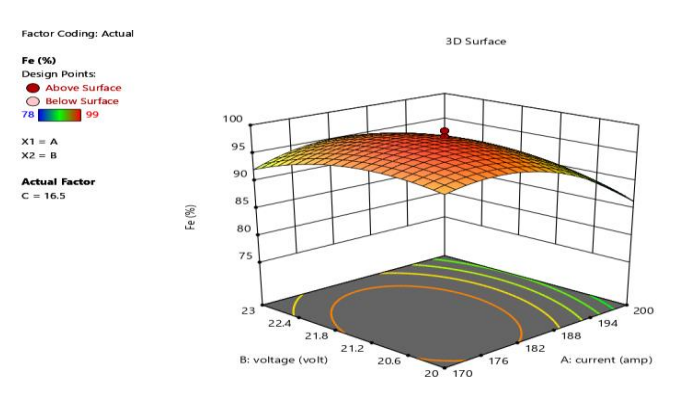


Fig. 5 Effect of current and voltage on Fe

Fig. 5 above shows the effect of current and voltage has on Fe. In studying the effects of gas flow rate and current on the Fe content, 3D surfaces plots presented in Fig. 6 was generated as follows.

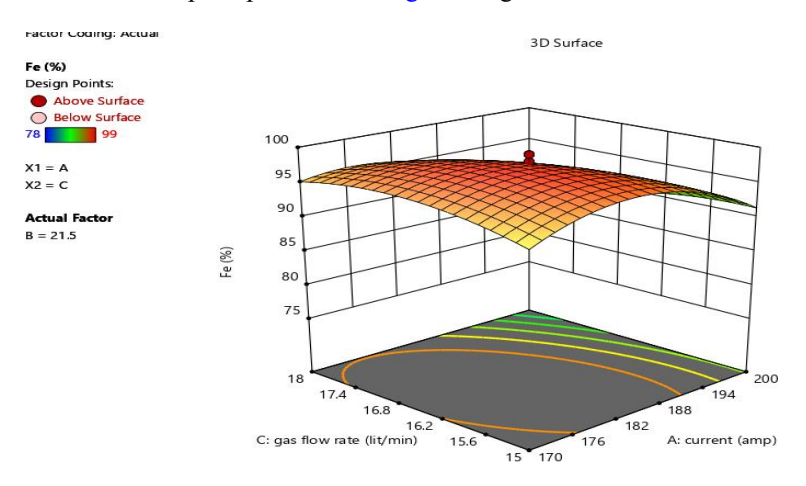


Fig. 6 Effect of current and gas flow rate on Fe

In studying the effects of gas flow rate and voltage on the Fe content 3D surface plots presented in Figure 7 was generated as follows:

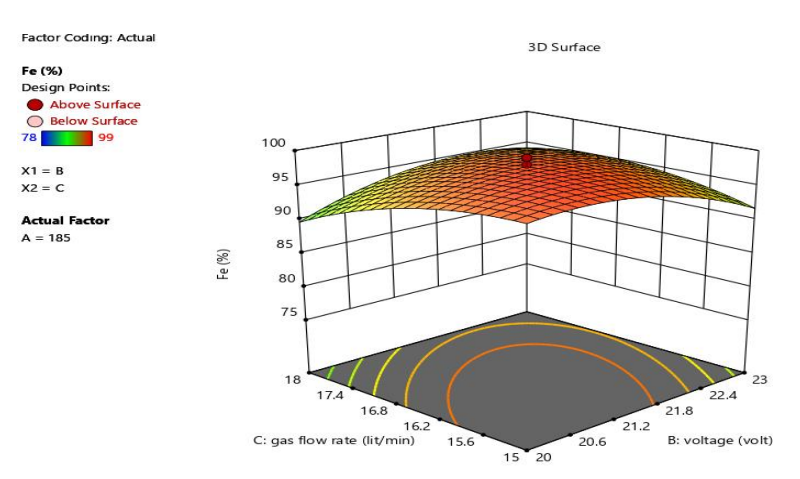


Fig. 7 Effect of voltage and gas flow rate on Fe

The 3D surface plots as observed in Figs. 5-7, shows the relationship between the input variables (current, voltage and gas flow rate) against the response variable, Fe. It is a 3-dimensional surface plot which was employed to give a clearer concept of the response surface. Although not as useful as the contour plot for establishing responses values and coordinates, this view may provide a clearer picture of the surface. As the color of the curved surface gets darker, the Fe content decreases proportionately. The presence of a colored hole at the middle of the upper surface gave a clue that more points lightly shaded for easier identification fell below the surface.

3.2 Modelling and Prediction of Fe using Artificial Neural Network (ANN)

In Matlab, APPS is selected, then Neural Net Fitting to begin the analysis process. To begin, we have to import the data initially loaded into Matlab into the Neural network fitting space. The improved second order method of gradient also known as Levenberg Marquardt Back Propagation training algorithm is selected as the best learning rule and was therefore adopted in designing the network architecture. The input layer of the network uses the hyparbolic targent (tan-sigmoid) transfer function to calculate the layer output from the network input while the output layer uses the linear (purelin) transfer function. The network generation process divides the input data into training data sets, validation and testing. For this study, 70% of the data was employed to perform the network training, 15% for validating the network while the remaining 15% was used to test the performance of the network at a maximum training cycle of 1000 epochs was used. Trainlm is a network training function that updates weight and bias values according to Levenberg-Marquardt optimization.

Trainlm is often the fastest back propagation algorithm in the toolbox, and is highly recommended as a first-choice supervised algorithm, although it does require more memory than other algorithms. The Artificial Neural Network architecture is 3-5-1, the network diagram generated for the prediction of Fe using the back propagation neural network is presented in Fig. 8.



Fig. 8 Model summary for predicting Fe

In the network training diagram of Figure 8, it was observed that the network performance was 211. Validation checks of six (6) was recorded out of six (6). However, this is expected since the issue of weight biased had been addressed via normalization of the raw data. A performance evaluation plot which shows the progress of training, validation and testing is presented in Fig. 9.

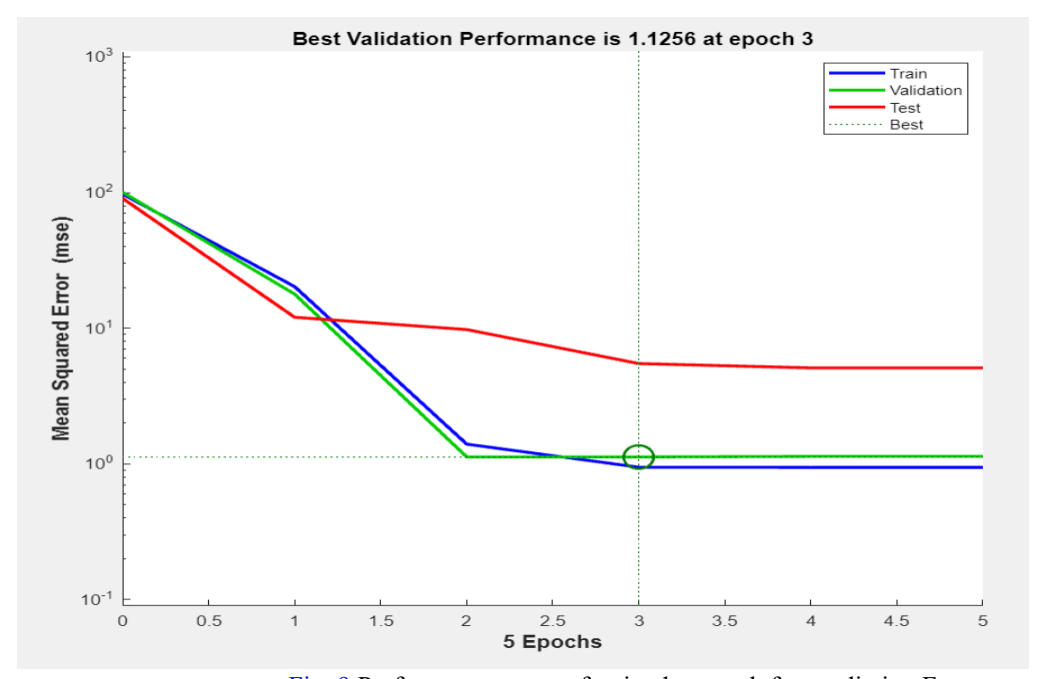


Fig. 9 Performance curve of trained network for predicting Fe

In the performance plot of Fig. 9, no evidence of over fitting was observed. In addition, similar trend was observed in the behaviour of the training, validation and testing curve which is expected since the raw data were normalized before use. Lower mean square error is a fundamental criterion used to determine the training accuracy of a network. An error value of 1.1256 at epoch 3 is evidence of a network with strong capacity to predict the Fe. The training state, which shows the gradient function, the training gain (Mu) and the validation check, is presented in Fig. 10.

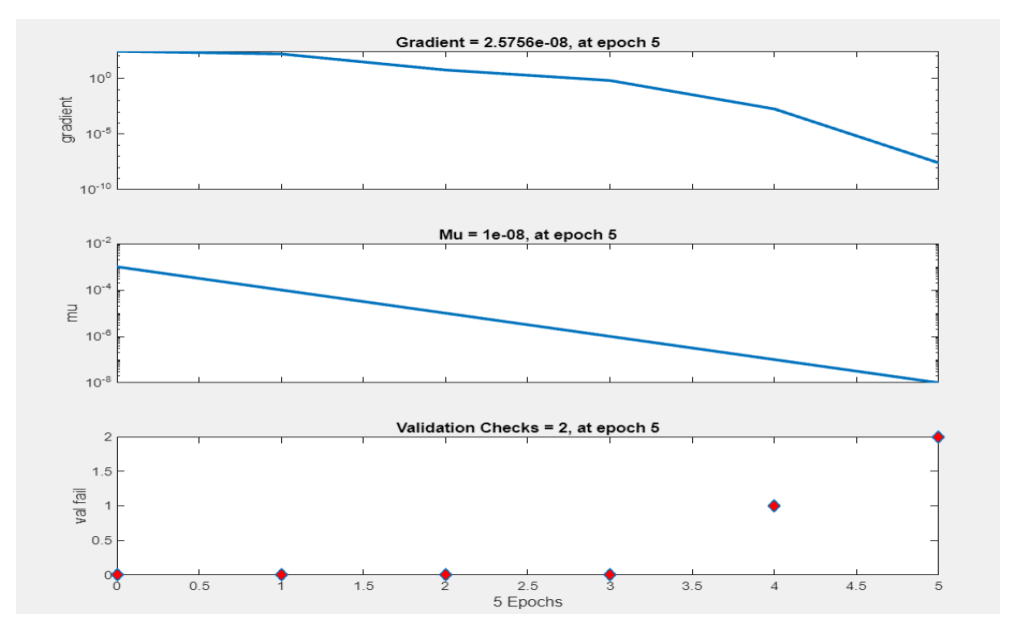


Fig. 10 Neural network training state for predicting Fe

Back propagation is a method used in artificial neural networks to calculate the error contribution of each neuron after a batch of data training. Technically, the neural network calculates the gradient of the loss function to explain the error contributions of each of the selected neurons. Lower error is better. Computed gradient value of 2.5756e-08 as observed in Figure 10 indicates that the error contributions of each selected neuron is very minimal. Momentum gain (Mu) is the control parameter for the algorithm used to train the neural network. It is the training gains and its value must be less than unity. Momentum gains of 1e-08 shows a network with high capacity to predict the Fe. The regression plot which shows the correlation between the input variables (current, voltage and gas flow rate) and the target variable Fe coupled with the progress of training, validation and testing is presented in Fig.11.

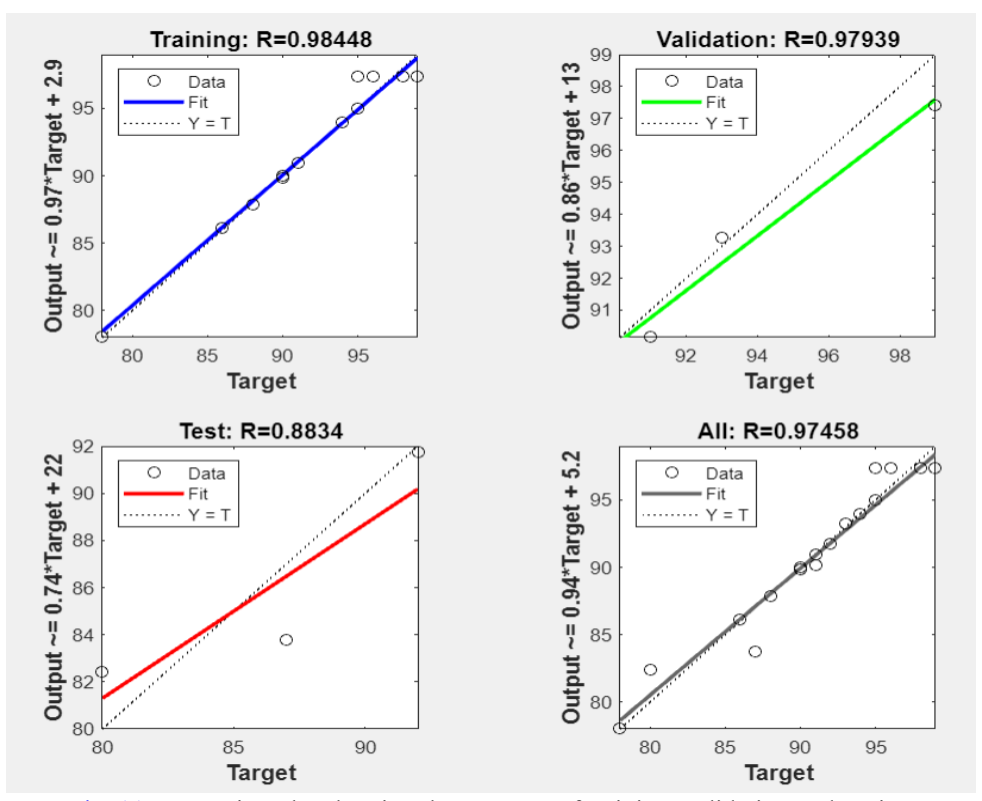


Fig. 11 Regression plot showing the progress of training, validation and testing

Based on the computed values of the correlation coefficient (R) as observed in Fig. 11, it was concluded that the network has been accurately trained and can be employed to predict the Fe. Table-5 below shows the ANN prediction for Fe.

Table-5	ANN	Prediction	for I	Fe
---------	-----	------------	-------	----

S/N	Current	Voltage	Gas flow rate	Fe	Fe_ANN
1	185	21.5	16.5	99	93
2	200	23	18	86	84
3	185	21.5	16.5	99	93
4	170	23	15	87	92
5	200	20	15	90	88
6	159.8	21.5	16.5	91	88
7	210.2	21.5	16.5	80	72
8	185	18.9	16.5	92	93
9	185	24.0	16.5	90	92
10	170	20	18	91	90
11	185	21.5	16.5	96	93
12	170	20	15	95	91
13	185	21.5	16.5	99	93
14	200	20	18	78	82
15	170	23	18	93	93
16	185	21.5	19	91	92
17	185	21.5	16.5	95	93
18	185	21.5	13.9	94	91
19	185	21.5	16.5	98	93
20	200	23	15	88	89

CONCLUSION

A close examination of the molten evaporation rate and droplet temperature required for Fe during globular to spray was experimented with carefully selecting the welding parameters using these factors; welding current, welding voltage and gas flow rate to predict and to optimize the evaporation rates of Fe alloys required for deep penetration using response surface method. The parameters having the most significant effect on Fe content and transfer modes are welding current, welding voltage and gas flow rate; to achieve a better weld with deep penetration and less spatter considering the transfer mode (spray), the current which controls the heat input should be controlled to range of about 185.175Amp, voltage of 20Volts and gas flow rate of 15.959 to give Fe of 96.484. The study shows that employing computational techniques such as the RSM and ANN for optimizing and predicting evaporation rates of Fe alloys considering droplet temperature in welding is a significant approach for enhancing weld quality and advancing manufacturing processes. The following conclusions can be deduced from this study:

(i). The findings of this study indicate that RSM is a highly efficient and reliable approach for prediction and optimisation of the output parameter (Fe) of TIG mild steel weld. The ability of RSM to offer a more exact interpretation of the experimental results seemed to be reasonable once the predicted R² and adjusted-R² had a good correlation, which was used to support the equation in the second-order polynomial model. This allows engineers to select optimum operating conditions to achieve accurate productivity and quality goals.

- (ii). Effective modelling and control of evaporation rates directly such as porosity and inclusions. By accurately predicting how droplet temperature impacts evaporation, the study provides a pathway to minimize such problems in welding and, consequently, to create a weld with better mechanical and structural properties.
- (iii). The integration of RSM and ANNs into welding analysis proves that there are significant possibilities of the same (for industrial applications). This optimisation method provides fast, data-driven process approach, offering a computationally efficient alternative to resource-intensive experimental and purely numerical techniques. Machine learning models, particularly ANN, delivered high predictive reliability with lower mean absolute errors, supporting robust process control with considerably reducing the number of unnecessary trial-and-error experiments.

The findings contribute to the knowledge required for the development of decentralized and intelligent welding systems by illustrating how more sophisticated computational techniques can be employed to re-conceptualize the evaluation and optimization of key welding parameters. This paves the way for robust, high-quality, and defect-minimized fabrication in industrial settings. Further studies should look into areas such as investigating the application of hybrid machine learning approaches and real-time monitoring in large-scale industrial welding environments, as well as using different alloy systems to validate and expand the predictive models.

CONFLICT OF INTEREST

The authors declare no conflict of interest.

REFERENCES

Abiodun, I.O. *et al.* (2019). Comprehensive Review of Artificial Neural Network Applications to Pattern Recognition. *IEEE Access*, 7, 158820–158846. doi: 10.1109/ACCESS.2019.2945545.

Baehr, S., Melzig, L., Bauer, D., Ammann, T., & Zaeh, M. F. (2018). Investigations of process by-products by means of Schlieren imaging during the powder bed fusion of metals using a laser beam. *Journal of Laser Applications*, 34(4)

Bunaziv, I., Akselsen, O. M., Ren, X., Nyhus, B., Eriksson, M., & Gulbrandsen-Dahl, S. (2021). A review on laser-assisted joining of aluminium alloys to other metals. *Metals*, 11(11), 1680

Cadiou, S., Courtois, M., Carin, M., Berckmans, W., & Le Masson, P. (2020). Heat transfer, fluid flow and electromagnetic model of droplets generation and melt pool behaviour for wire arc additive manufacturing. *International Journal of Heat and Mass Transfer*, 148, 119102,

Chen, L., Nishida, K., Murakami, K., Liu, L., Kobayashi, T., Li, Z., & Sekimura, N. (2018). Effects of solute elements on microstructural evolution in Fe-based alloys during neutron irradiation following thermal ageing. *Journal of Nuclear Materials*, 498, 259-268

Chen, F. F., Xiang, J., Thomas, D. G., & Murphy, A. B. (2020). Model-based parameter optimization for arc welding process simulation. *Applied mathematical modelling*, *81*, 386-400

Cho, W. I., & Na, S. J. (2021). Impact of driving forces on molten pool in gas metal arc welding", Welding in the World, 65 (9), 1735-1747, 2021

Fotovvati, B., Wayne, S. F., Lewis, G., & Asadi, E. (2018). A review on melt-pool characteristics in laser welding of metals. *Advances in Materials Science and Engineering*

Ghaini, M., Moosavy, F.M., Sheikhi, H.N., Torkamany, M. J., & Moradi, M. (2020). The relation between magnesium evaporation and laser absorption and weld penetration in pulsed laser welding of aluminum alloys: Experimental and numerical investigations. *Optics & Laser Technology*, 128, 106170

Indhu, R., Soundarapandian, S., & Vijayaraghavan, L. (2018). Yb: YAG laser welding of dual phase steel to aluminium alloy. *Journal of Materials Processing Technology*, 262, 411-421,

Kaiser, E., Kutz, J. N., & Brunton, S. L. (2018). Sparse identification of nonlinear dynamics for model predictive control in the low-data limit. *Proceedings of the Royal Society A*, 474(2219), 20180335

Kim, J., Kim, D.G., Ryu, K.H. (2025). Piecewise Response Surface Methodology for Enhanced Modeling and Optimization of Complex Systems. *Korean Journal of Chemical Engineering*, 42(3), 537–545. doi: 10.1007/s11814-024-00362-4

Lian, L., Chen, T. (2024). Research on Complex Data Mining Analysis and Pattern Recognition Based on Deep Learning. *Journal of Computing and Electronic Information Management*, 12(3), 37–41. doi: 10.54097/i4jfi9aa

Mamat, S. B., Tashiro, S., Tanaka, M., & Yusoff, M. (2018). Study on factors affecting the droplet temperature in plasma MIG welding process. *Journal of Physics D: Applied Physics*, 5(13), 135206

Martin, Aiden A., Nicholas P. Calta, Joshua A. Hammons, Saad A. Khairallah, Michael H. Nielsen, Richard M. Shuttlesworth, Nicholas Sinclair (2019). Ultrafast dynamics of laser-metal interactions in additive manufacturing alloys captured by in situ X-ray imaging. *Materials Today Advances*, 1, 100002, 2019.

Oyejide, O.J., Faiz A., Ayoub M., Okwu M.O (2024). Decision Support Analytical Approach on the Process Variables influencing gasoline yield in the Fluid Catalytic Cracking Unit'. 5th International Conference on Industry 4.0 and Smart Manufacturing (ISM). *Procedia Computer Science, ScienceDirect*, 232, 3044–3053. DOI: 10.1016/j.procs.2024.02.120.

Oyejide, O.J., Faiz A., Shahrul B.K., Okwu M.O., Amadhe F., Adeleke T. B., Anjorin R., El-fakih M. A. (2025). Novel Stacked-Model Configuration for Merox-Treated Gasoline Yield Prediction Synergized with EMMS-CFD Hydrodynamic Analysis. *Knowledge-Based Systems Journal. KNOSYS*

Paul, A., Dhar, P. (2024). Predicting sessile droplet evaporation kinetics via cascaded deep networks and tree-based machine learning approach. *Phys. Fluids*, 36(9). doi: 10.1063/5.0230332

Rawa, M., Dehkordi, M. H. R., Javad-Kalbasi, M., Abu-Hamdeh, N., Azimy, H. (2023). Using the numerical simulation and artificial neural network (ANN) to evaluate temperature distribution in pulsed laser welding of different alloys. *Eng. Appl. Artif. Intell.*, 126, 107025. doi: 10.1016/j.engappai.2023.107025.

Slobodyan, M. (2021). Resistance, electron-and laser-beam welding of zirconium alloys for nuclear applications: A review. *Nuclear Engineering and Technology*, 53(4), 1049-1078

Veza, I., Spraggon, M., Fattah, I.M.R., Idris, M. (2023). Response surface methodology (RSM) for optimizing engine performance and emissions fueled with biofuel: Review of RSM for sustainability energy transition. *Results in Engineering*, 18. doi: 10.1016/j.rineng.2023.101213

Wang, J., Zhu, R., Liu, Y., & Zhang, L. (2023). Understanding melt pool characteristics in laser powder bed fusion: An overview of single-and multi-track melt pools for process optimization. *Advanced Powder Materials*, 2(4), 100137

Zhang, Y., Chen, Y., Yu, D., Sun, D., & Li, H. (2020). A review paper on effect of the welding process of ceramics and metals. *Journal of Materials Research and Technology*, 9(6), 16214-16236

Zhang, D., Wei, Y., Zhan, X., Chen, J., Li, H., Wang, Y. (1993). Numerical simulation of keyhole behaviors and droplet transfer in {laser-MIG} hybrid welding of Invar alloy. *Int. J. Numer. Methods Heat Fluid Flow*, 28(9), 1974–1993. doi: 10.1108/HFF-07-2017-0266.

Zhang, M., Han, Y., Jia, C., Zheng, Z., Li, H., & Wu, C. (2022). Improving the microstructures and mechanical properties with nano-Al2O3 treated wire in underwater submerged arc welding. *Journal of Manufacturing Processes*, 74, 40-51

Zhu, C., Cheon, J., Tang, X., Na, S. J., & Cui, H. (2018). Molten pool behaviors and their influences on welding defects in narrow gap GMAW of 5083 Al-alloy. *International Journal of Heat and Mass Transfer*, 126, 1206-1221